J. Math. Computer Sci., 40 (2026), 84–100

Online: ISSN 2008-949X

Journal of Mathematics and Computer Science

Journal Homepage: www.isr-publications.com/jmcs

A numerical study of nonlinear mixed Volterra-Fredholm integral equations using Toeplitz matrix method

M. E. Nasr[a], Sahar M. Abusalim[a], M. A. Abdou[b], K. M. Khalil[a], M. A. Abdel-Aty[c,*]

[a]Department of Mathematics, College of Science, Jouf University, Sakaka, Saudi Arabia.

[b]Department of Mathematics, Faculty of Education, Alexandria University, Alexandria, Egypt.

[c]Department of Mathematics and Computer Science, Faculty of Science, Benha University, Benha 13518, Egypt.

Abstract

It is known that integral equations, whether linear or nonlinear, and whether the kernel is continuous or discontinuous, play a major role in explaining physical and engineering phenomena. The importance of these equations appears when calculating the effect of time and its impact on the solution. This importance increases if the study is based on nonlinear integral equations with a singular kernel. In this study, a nonlinear equation was assumed, and the effect of time during a certain period was studied, with the assumption of the singular kernel of the integral equation in a general form. All the previous singular kernels can be derived from it as special cases. Many methods, whether semi-analytical or numerical, can find solutions to integral equations. However, these methods fail to find the solution when the kernel is singular. If we deal with the orthogonal polynomial method, it treats each type of singular kernel as an independent case. Therefore, the authors in this research used the Toeplitz matrix method (TMM), considering the kernel in a general form and deriving special cases as applications of the method. Here, the existence and uniqueness of the solutions of the second-kind nonlinear mixed Volterra-Fredholm integral equation (NMV-FIE) are discussed. The integral operator is shown to be normal and continuous. We then derive a numerically solvable nonlinear algebraic system (NLAS) using the TMM. The Banach fixed point theorem is used to prove that this NLAS is solvable. When the kernel takes a logarithmic and Hilbert kernels, numerical examples are discussed and the estimation error, in each case, is calculated. Some numerical experiments are performed to show the efficiency of the presented approach, and all results are performed by using the program Wolfram Mathematica 11.

Keywords: Banach fixed point theorem, nonlinear mixed Volterra-Fredholm integral equation, integral operator, Toeplitz matrix method.

2020 MSC: 45G10, 45P05, 45H10, 65R20.

1. Introduction

This paper uses a new numerical approach to solve the nonlinear mixed Volterra-Fredholm integral equation (NMV-FIE) as follows:

$$\Theta(x,t) = f(x,t) + \lambda \int_0^t \int_\Omega F(t,\tau) k(|u-v|) \varpi(\tau, y, \Theta(y,\tau)) dy d\tau, \tag{1.1}$$

*Corresponding author

Email addresses: menasr@ju.edu.sa (M. E. Nasr), sabosalem@ju.edu.sa (Sahar M. Abusalim), abdella_777@yahoo.com (M. A. Abdou), kmshalaby@ju.edu.sa (K. M. Khalil), mohammed.abdallah@fsc.bu.edu.eg (M. A. Abdel-Aty)

doi: 10.22436/jmcs.040.01.06

Received: 2024-10-16 *Revised:* 2025-01-06 *Accepted:* 2025-04-07

which λ is a constant parameter and the function $\Theta(x,t)$ is called the unknown potential function in the Banach space $L_2(\Omega) \times C[0,T]$, $0 \leqslant T < 1$. The domain of integration with regard to the position is Ω and the time $t \in [0,T]$. The kernel $F(t,\tau)$ is a continuous in $C[0,T]$ and the given function $f(x,t)$ is continuous in the space $L_2(\Omega) \times C[0,T]$. Also, the singular kernel of position $k(|u-v|)$ belongs to $L_2(\Omega)$ and a discontinuous function.

Integral equations often appear in mathematical modeling, which has a mathematical theory of elasticity [37], economics [15], quantum mechanics[25], fluid mechanics [41], generalized potential theory [9], population genetics [11], nonlinear equations for boundary value theory [8, 11], spectral relationships in laser theory [20], contact problems between two elastic material layers [6], radiation [26], and electromagnetic and electrodynamics [12, 44]. The Volterra-Fredholm type integral equations are difficult to solve exactly, hence we usually use numerical techniques [18, 29, 35, 38]. To obtain the approximate solution of the linear and nonlinear integral equations of the Volterra-Fredholm type, many computational methods have recently been developed. Taylor series expansion is an important technique developed in [13, 27]. In certain cases, the Adomian decomposition method [2] and the Homotopy analysis method [5] are two powerful methods that often provide the exact solution. Many computing methods have been developed to solve the NMV-FIE given by equation (1.1), including the Legendre polynomials [14], Bernstein polynomials [19], Alpert's multiwavelet bases [24], Laguerre and Hermite polynomials [4], conflict-type wavelets [42], Homotopy analysis methods [21], Runge-Kutta method and Block-by-block method [7], modified homotopy perturbation method [17], optimal perturbation iteration method [16], Chebyshev wavelets polynomials [40], Picard iteration method [28], Adomian decomposition method [1], Lagrange polynomials [39], Lagrange-collocation method [34], Legendre polynomials [36], Tau-collocation method [22], separation of variables method [33], Collocation method [31], Hat functions [23], hybrid functions method [3], modified Taylor's method [30], Taylor polynomial method [43], operational matrices [32], and degenerate kernel method [10]. Our main goal of the study is to discuss the existence and uniqueness of the solutions of the equation (1.1), and determine the numerical solution to the problem given by this equation, for which we have devised a new and accurate method.

In this paper, we consider the nonlinear mixed Volterra-Fredholm integral equation of the second type with a discontinuous kernel. We use a numerical method to transform the NMV-FIE into a nonlinear algebraic system, where the existence and the uniqueness of the solution of the NLAS can be discussed and proved using the Banach fixed point theorem. To find the numerical solution of the NLAS, we used the Toeplitz matrix method.

2. Special cases

Many special cases can be derived from the mixed integral equation as follows.

(1) Let, in (1.1), $\varpi(\tau, y, \Theta(y,\tau)) = \Theta(y,\tau)$ to have

$$\Theta(x,t) = f(x,t) + \lambda \int_0^t \int_\Omega F(t,\tau) k(|u-v|) \Theta(y,\tau) dy d\tau. \tag{2.1}$$

Equation (2.1) represents a mixed linear integral equation of the Volterra-Fredholm type of the second kind with a continuous time-specific kernel and a general anomalous position-specific kernel. Equation (2.1) plays an important role in understanding many mathematical and engineering applications, especially in communication problems of all different types, which depend entirely on the shape of the kernel.

(2) The kernel of position of equation (1.1) or (2.1) can take the following forms.
   (2.i) Logarithmic kernel $k(|u-v|) = \ln(|u-v|)$.
   (2.ii) Carleman kernel $k(|u-v|) = |u-v|^{-n}$, $0 \leqslant n < 1$.
   (2.iii) The relation between logarithmic kernel and Caleman function is

$$\ln(|u-v|) = |u-v|^n \ln(|u-v|)|u-v|^{-n} = H(u,v)|u-v|^{-n}, \quad 0 \leqslant n < 1,$$

   where $H(u,v)$ is continuous function.

(2.iv) Cauchy kernel $k(|u-v|) = 1/|u-v|$.
(2.v) Strong singular kernel $k(|u-v|) = 1/(u-v)^2$.
(2.vi) Hilbert kernel $k(|u-v|) = \cot \frac{|u-v|}{2}$.

Many different methods, whether numerical or semi-analytical, have been used to solve equation (1.1) or equation (2.1) with one of the different kernels mentioned above. However, the Toeplitz matrix method is distinguished by the fact that it applies to the general kernel case, in general. As for the cases derived from it, we consider them special applications of the original kernel.

3. Existence and uniqueness solution of NMV-FIE (1.1)

We make the following assumptions to discuss the existence and uniqueness solution of NMV-FIE (1.1).

(i) The kernel $k(|u-v|)$ satisfies $\left[\int_\Omega \int_\Omega k^2(|u-v|)dxdy\right]^{\frac{1}{2}} = D$, where D is a constant.
(ii) The positive function of time, $F(t,\tau)$, satisfies the continuity condition $|F(t,\tau)|_{C[0,T]} \leqslant A$, $\forall t,\tau \in [0,T]$, where A is a constant.
(iii) The norm of known function $f(x,t)$ in $L_2(\Omega) \times C[0,T]$, $T < 1$ space is

$$\|f(x,t)\| = \max_{0\leqslant t\leqslant T<1} \left| \int_0^t \left[\int_\Omega f^2(x,\tau)dx \right]^{\frac{1}{2}} d\tau \right| = G,$$

where G is a constant.
(iv) The known function $\varpi(t,x,\Theta(x,t))$, for the constants $B > B_1$ and $B > B_2$, satisfies:
(iv-a) $|\varpi(t,x,\Theta(x,t))| \leqslant B_1|\Theta(x,t)|$;
(iv-b) $|\varpi(t,x,\Theta_1(x,t)) - \varpi(t,x,\Theta_2(x,t))| \leqslant B_2|\Theta_1(x,t) - \Theta_2(x,t)|$.

Theorem 3.1. *If the conditions* (i)-(iv-b) *are satisfied, and*

$$(A\lambda BTD) < 1, \quad \textit{where} \quad T = \max_{0<t\leqslant T} |t|,$$

then NMV-FIE (1.1) *has a unique solution* $\Theta(x,t)$ *in the Banach space* $L_2(\Omega) \times C[0,T]$.

Proof. We employ the successive approximation approach (*Picard's method*) to demonstrate this theorem. As $\{i\}$ goes to ∞, a sequence of functions $\{\Theta_i(x,t)\}$ can be formed as a convergent solution for NMV-FIE (1.1), hence, $\Theta(x,t) = \lim_{i\to\infty} \Theta_i(x,t)$, where

$$\Theta_i(x,t) = \sum_{j=0}^{i} \Psi_j(x,t), \ t \in [0,T], \ i = 0,1,2,\ldots,$$

where the functions $\Psi_j(x,t)$, $j = 0,1,\ldots,i$ are continuous functions and take the form:

$$\left.\begin{aligned} \Psi_i(x,t) = \Theta_i(x,t) - \Theta_{i-1}(x,t) \\ \Psi_0(x,t) = f(x,t) \end{aligned}\right\} \tag{3.1}$$

To establish the previous theorem, we need to take into consideration the following lemmas.

Lemma 3.2. *If the series* $\sum_{j=0}^{i} \Psi_j(x,t)$ *is uniformly convergent, then* $\Theta(x,t)$ *represents a solution of NMV-FIE* (1.1).

Proof. We design a series described by $\Theta_i(x,t)$,

$$\Theta_i(x,t) = f(x,t) + \lambda \int_0^t \int_\Omega F(t,\tau)k(|x-y|)\varpi(\tau,y,\Theta_{i-1}(y,\tau))dyd\tau.$$

Next, we obtain

$$\Theta_i(x,t) - \Theta_{i-1}(x,t) = \lambda \int_0^t \int_\Omega F(t,\tau)k(|x-y|)[\varpi(\tau,y,\Theta_{i-1}(y,\tau)) - \varpi(\tau,y,\Theta_{i-2}(y,\tau))]dyd\tau.$$

By applying the norm's characteristics to equation (3.1), we can obtain

$$\|\Psi_i(x,t)\| = |\lambda| \left\| \int_0^t \int_\Omega F(t,\tau)k(|x-y|)[\varpi(\tau,y,\Theta_{i-1}(y,\tau)) - \varpi(\tau,y,\Theta_{i-2}(y,\tau))]dyd\tau \right\|.$$

Using (iv-b), we have

$$\begin{aligned}
\|\Psi_i(x,t)\| &\leqslant |\lambda| \left\| \int_0^t \int_\Omega F(t,\tau)k(|x-y|)Z(\tau,y)|\Theta_{i-1}(y,\tau) - \Theta_{i-2}(y,\tau)|dyd\tau \right\| \\
&\leqslant |\lambda| \left\| \int_0^t \int_\Omega F(t,\tau)k(|x-y|)Z(\tau,y)|\Psi_{i-1}(y,\tau)|dyd\tau \right\| \\
&\leqslant |\lambda B| \left\| \int_0^t \int_\Omega F(t,\tau)k(|x-y|)|\Psi_{i-1}(y,\tau)|dyd\tau \right\|.
\end{aligned}$$

Using conditions (i) and (ii), we obtain

$$\|\Psi_i(x,t)\| \leqslant [A\lambda BTD]\|\Psi_{i-1}(x,t)\|. \tag{3.2}$$

Using condition (iii) and $i = 1$, we obtain from formula (3.2):

$$\|\Psi_1(x,t)\| \leqslant [A\lambda BTD]\|\Psi_0(x,t)\| \leqslant [A\lambda BTD]G.$$

Then, by induction, we have

$$\|\Psi_i(x,t)\| \leqslant Y^i G,\ Y = [A\lambda BTD] < 1,\ i = 0,1,2,\ldots.$$

This leads us to conclude that there is a convergent solution for the sequence $\Theta_i(x,t)$. In this way, we have for $i \to \infty$,

$$\begin{aligned}
\Theta(x,t) &= \lim_{i\to\infty} \left(f(x,t) + \lambda \int_0^t \int_\Omega F(t,\tau)k(|x-y|)\varpi(\tau,y,\Theta_i(y,\tau))dyd\tau \right) \\
&= f(x,t) + \lambda \int_0^t \int_\Omega F(t,\tau)k(|x-y|)\varpi(\tau,y,\Theta(y,\tau))dyd\tau.
\end{aligned}$$

Consequently, it is proven that there is an NMV-FIE solution (1.1). □

Lemma 3.3. *The function $\Theta(x,t)$ represents a unique solution of NMV-FIE (1.1).*

Proof. Assuming that there is another continuous solution $\Theta^*(x,t)$ of NMV-FIE (1.1), we may demonstrate that $\Theta(x,t)$ is the only solution, then we get

$$\Theta^*(x,t) = f(x,t) + \lambda \int_0^t \int_\Omega F(t,\tau)k(|x-y|)\varpi(\tau,y,\Theta^*(y,\tau))dyd\tau,$$

and

$$\Theta(x,t)-\Theta^*(x,t)=\lambda\int_0^t\int_\Omega F(t,\tau)k(|x-y|)[\varpi(\tau,y,\Theta(y,\tau))-\varpi(\tau,y,\Theta^*(y,\tau))]dyd\tau.$$

By using the norm's properties, we have

$$\|\Theta(x,t)-\Theta^*(x,t)\|\leqslant|\lambda|\left\|\int_0^t\int_\Omega F(t,\tau)k(|x-y|)[\varpi(\tau,y,\Theta(y,\tau))-\varpi(\tau,y,\Theta^*(y,\tau))]dyd\tau\right\|.$$

Using (iv-b), we have

$$\begin{aligned}\|\Theta(x,t)-\Theta^*(x,t)\|&\leqslant|\lambda|\left\|\int_0^t\int_\Omega F(t,\tau)k(|x-y|)Z(\tau,y)[\Theta(y,\tau)-\Theta^*(y,\tau)]dyd\tau\right\|\\&\leqslant|\lambda B|\left\|\int_0^t\int_\Omega F(t,\tau)k(|x-y|)[\Theta(y,\tau)-\Theta^*(y,\tau)]dyd\tau\right\|.\end{aligned}$$

Using conditions (i) and (ii), we have

$$\|\Theta(x,t)-\Theta^*(x,t)\|\leqslant[A\lambda BTD]\|\Theta(x,t)-\Theta^*(x,t)\|\leqslant Y\|\Theta(x,t)-\Theta^*(x,t)\|,\quad Y<1.$$

If $\|\Theta(x,t)-\Theta^*(x,t)\|\neq0$, then the last formula yields $Y\geqslant1$ which is a contradiction. Therefore, $\|\Theta(x,t)-\Theta^*(x,t)\|=0$ and it is implied that $\Theta(x,t)=\Theta^*(x,t)$ which means the solution is unique. □

4. Normality and continuity of an integral operator

The successive approximation method (Picard's method) is characterized by the fact that it gives directly the convergence of the solution and that there is a converging solution and then it follows the study of whether this solution is unique or not. This method is not suitable at two important points:

(1) if the integral equation is of the first kind;
(2) if the integral equation is homogeneous.

Therefore, it is better for the study to apply the fixed point theorem. At first, the reduced NMV-FIE (1.1) will be mentioned in its integral operator form to demonstrate its normality and continuity:

$$\overline{V}\Theta(x,t)=f(x,t)+V\Theta(x,t),\quad V\Theta(x,t)=\lambda\int_0^t\int_\Omega F(t,\tau)k(|x-y|)\varpi(\tau,y,\Theta(y,\tau))dyd\tau.\tag{4.1}$$

Then, we state the following.

Lemma 4.1. *Under the conditions* (i)-(iv-a) *the integral operator* $\overline{V}\Theta(x,t)$ *maps the space* $L_2(\Omega)\times C[0,T], T<1$, *into itself.*

Proof. Consider the normality of equation (4.1), to have

$$\|V\Theta(x,t)\|\leqslant|\lambda|\|F(t,\tau)\|k(|x-y|)|\left\|\int_0^t\int_\Omega\varpi(\tau,y,\Theta(y,\tau))dyd\tau\right\|.$$

Applying the principal conditions, we have

$$\|V\Theta(x,t)\|\leqslant[A|\lambda|BTD]\|\Theta(x,t)\|.\tag{4.2}$$

From (4.1) and (4.2) we have

$$\|\overline{V}\Theta(x,t)\|\leqslant\|f(x,t)\|+\|V\Theta(x,t)\|\leqslant G+[A|\lambda|BTD]\|\Theta(x,t)\|.$$

The above inequality leads us to decide that the ball S_r is mapped into itself by the operator $\overline{V}$, wherever $r=\frac{G}{1-A|\lambda|BTD}$. Since $r>0$, $G>0$. This leads us to decide $A|\lambda|BTD<1$. Moreover, inequality (4.2) leads us to decide that the operator $V\Theta(x,t)$ is bounded. □

Lemma 4.2. *Under the conditions* (i)-(iv-b) *the integral operator* $\overline{V}\Theta(x,t)$ *is continuous. Moreover, under the condition* $A|\lambda|BTD < 1$, *the same operator is a contraction.*

Proof. Assuming that the integral operator form (4.1) is satisfied by the two functions $\Theta_1(x,t)$, $\Theta_2(x,t)$ in the space $L_2(\Omega) \times C[0,T]$, then

$$\overline{V}\Theta_1 = f(x,t) + \lambda \int_0^t \int_\Omega F(t,\tau)k(|x-y|)\varpi(\tau,y,\Theta_1(y,\tau))dyd\tau.$$

The function $\Theta_2(x,t)$ of $\Theta_1(x,t)$ can be subtracted to obtain $\overline{V}\Theta_1 - \overline{V}\Theta_2 = \overline{V}[\Theta_1 - \Theta_2]$. Using conditions (i), (ii), (iv-b), and the norm's properties, we get

$$\|\overline{V}[\Theta_1 - \Theta_2]\| \leqslant [A\lambda BTD]\|\Theta_1 - \Theta_2\|,$$

hence, we obtain

$$\|\overline{V}[\Theta_1 - \Theta_2]\| \leqslant Y\|\Theta_1 - \Theta_2\|, \quad Y < 1. \tag{4.3}$$

Inequality (4.3) leads to the continuity of the integral operator $\overline{V}$. Likewise, $\overline{V}$ is a contraction operator in the space $L_2(\Omega) \times C[0,T]$. Banach's fixed point theorem remarks that $\overline{V}$ includes a unique fixed point. If the normality and continuity of the integral operator are employed, then the existence and uniqueness of the reduced NMV-FIE (1.1) are approved. □

5. The Toeplitz matrix method (TMM)

The Toeplitz matrix method is distinguished from all numerical and semi-analytical methods by the fact that it collects all the anomalous kernels in one general form. Then the cases to be studied are considered as special cases of the problem kernel. For example, the logarithmic kernel, the Carleman kernel, the Hilbert kernel, the Cauchy kernel, and also the strongly anomalous kernel are all special cases of the general kernel of the Toeplitz matrix method. What is also more important is that the anomalous integrals, after using the technique, are transformed into ordinary integrals that are easy to solve.

We will now talk about the numerical solution of NMV-FIE (1.1) using TMM, and $\Omega = [-a, a]$. For this, we write MV-FIE (1.1) in the form

$$\Theta(x,t) = f(x,t) + \lambda \int_0^t \int_{-a}^a F(t,\tau)k(|x-y|)\varpi(\tau,y,\Theta(y,\tau))dyd\tau,$$

the integral term can be expressed as follows for this:

$$\int_{-a}^a k(|x-y|)\varpi(\tau,y,\Theta(y,\tau))dy = \sum_{m=-M}^{M-1} \int_{M\rho}^{M\rho+\rho} k(|x-y|)\varpi(\tau,y,\Theta(y,\tau))dy, \quad \rho = \frac{a}{M}. \tag{5.1}$$

The integral in Eq. (5.1) on the right side can be expressed as

$$\begin{aligned} &\int_{M\rho}^{M\rho+\rho} k(|x-y|)\varpi(\tau,y,\Theta(y,\tau))dy \\ &\qquad = X_m(x)\varpi(\tau,M\rho,\Theta(M\rho,\tau)) + Y_m(x)\varpi(\tau,M\rho+\rho,\Theta(M\rho+\rho,\tau)) + R, \end{aligned} \tag{5.2}$$

where R is the estimate error and $X_m(x)$ and $Y_m(x)$ are arbitrary functions that need to be found. Using the Toeplitz matrix technique, we can calculate $X_m(x)$ and $Y_m(x)$ by substituting $\Theta(y,\tau) = \tau$ and $\Theta(y,\tau) = y\tau$, respectively, in Eq. (5.2). We are able to solve this set of equations for $X_m(x)$ and $Y_m(x)$ if R is taken to be negligible; the formula (5.1) becomes

$$\int_{-a}^a k(|x-y|)\varpi(\tau,y,\Theta(y,\tau))dy = \sum_{m=-M}^{M} U_m(x)\varpi(\tau,m\rho,\Theta(m\rho,\tau)),$$

where

$$U_m(x) = \begin{cases} X_M(x), & m = -M, \\ X_m(x) + Y_{m-1}(x), & -M < m < M, \\ Y_{M-1}(x), & m = M. \end{cases}$$

As a result, the form of the integral Eq. (1.1) is

$$\Theta(x,t) = f(x,t) + \lambda \int_0^t F(t,\tau) \sum_{m=-M}^{M} U_m(x)\varpi(\tau, m\rho, \Theta(m\rho,\tau))d\tau.$$

Let $x = n\rho$, $-M \leqslant n \leqslant M$, then the system of Fredholm integral equations that follows is obtained:

$$\Theta(n\rho,t) = f(n\rho,t) + \lambda \int_0^t F(t,\tau) \sum_{m=-M}^{M} U_m(n\rho)\varpi(\tau, m\rho, \Theta(m\rho,\tau))d\tau. \tag{5.3}$$

6. System of nonlinear algebraic equations

The solution of equation (5.3) is usually reduced to a system of nonlinear algebraic equations by using the quadrature method [4]. We divide the interval $[0,T]$, $0 \leqslant t \leqslant T$, as $0 = t_0 < t_1 < \cdots < t_l < \cdots < t_L = T$, where $t = t_l$, $l = 0,1,\ldots,L$, to get

$$\Theta(n\rho,t_l) = f(n\rho,t_l) + \lambda \int_0^{t_l} F(t_l,\tau) \sum_{m=-M}^{M} U_m(n\rho)\varpi(\tau, m\rho, \Theta(m\rho,\tau))d\tau, \tag{6.1}$$

and the following are the terms for the Volterra integrals:

$$\begin{aligned} &\int_0^{t_l} F(t_l,\tau) \sum_{m=-M}^{M} U_m(n\rho)\varpi(\tau, m\rho, \Theta(m\rho,\tau))d\tau \\ &\quad \approx \sum_{i=0}^{l} \omega_i F(t_l,t_i) \sum_{m=-M}^{M} U_m(n\rho)\varpi(t_i, m\rho, \Theta(m\rho,t_i)). \end{aligned} \tag{6.2}$$

Using Eq. (6.2) in Eq. (6.1), we obtain

$$\Theta(n\rho,t_l) = f(n\rho,t_l) + \lambda \sum_{i=0}^{l} \omega_i F(t_l,t_i) \sum_{m=-M}^{M} U_m(n\rho)\varpi(t_i, m\rho, \Theta(m\rho,t_i)).$$

And then using the notations $\Theta(n\rho,t_l) = \Theta_{nl}$, $F(t_l,t_i) = F_{li}$, $U_m(n\rho) = U_{mn}$, we obtain the following system of nonlinear algebraic equations:

$$\Theta_{nl} = f_{nl} + \lambda \sum_{i=0}^{l} \omega_i F_{li} \sum_{m=-M}^{M} U_{mn}\varpi_{im}(\Theta_{mi}). \tag{6.3}$$

One way to express the matrix U_{mn} is as $U_{mn} = H_{mn} - T_{mn}$, where

$$H_{mn} = X_m(n\rho) + Y_{m-1}(n\rho), \quad -M \leqslant m,n \leqslant M,$$

which is an order $2M+1$ Toeplitz matrix, and

$$T_{mn} = \begin{cases} Y_{-M-1}(n\rho), & m = -M, \\ 0, & -M < m < M, \\ X_M(n\rho), & m = M. \end{cases}$$

7. The existence of a unique solution of the system of nonlinear algebraic equations

In this part, we will provide evidence for the existence of the unique solution to the system of nonlinear algebraic equations (6.3) under certain conditions and obtain the numerical solution's truncation error. These goals can be attained with the use of the following theorems.

Theorem 7.1. *Under the following conditions:*

(1) *the matrix* $\left(\sum_{m=-M}^{M} |U_{mn}|^2\right)^{\frac{1}{2}} \leqslant D$;

(2) $\left(\sum_{i=0}^{l} |\omega_i F_{li}|^2\right)^{\frac{1}{2}} \leqslant A$;

(3) $|g_{nl}| \leqslant G$;

(4) *the known function* $\varpi_{im}(\Theta_{mi})$, *for the constants* $B > B_1$ *and* $B > B_2$, *satisfies*

(a) $|\varpi_{im}(\Theta_{mi})| \leqslant B_1|\Theta_{mi}|$;

(b) $|\varpi_{im}(\Theta_{mi,1}) - \varpi_{im}(\Theta_{mi,2})| \leqslant B_2|\Theta_{mi,1} - \Theta_{mi,2}|$.

The system of nonlinear algebraic equations (6.3) *has a unique solution.*

Proof. To establish the theorem, we express the system of nonlinear algebraic equations (6.3) in the following operator form:

$$\overline{V}\Theta_{nl} = f_{nl} + \lambda \sum_{i=0}^{l} \omega_i F_{li} \sum_{m=-M}^{M} U_{mn}\varpi_{im}(\Theta_{mi}). \tag{7.1}$$

□

Lemma 7.2. *Under the conditions* (1)-(4-a), *the operator* $\overline{V}$ *defined by* (7.1) *maps the space* ℓ_2 *into itself.*

Proof. From (7.1), we obtain:

$$\|\overline{V}\Theta_{nl}\|_{\ell_2} \leqslant \|f_{nl}\|_{\ell_2} + \|\lambda \sum_{i=0}^{l} \omega_i F_{li} \sum_{m=-M}^{M} U_{mn}\varpi_{im}(\Theta_{mi})\|_{\ell_2}.$$

Following application of conditions (1)-(4-a), the formula above takes on the following form:

$$\|\overline{V}\Theta_{nl}\|_{\ell_2} \leqslant G + |\lambda|AD\|\varpi_{im}(\Theta_{mi})\|_{\ell_2} \leqslant G + Y\|\Theta_{nl}\|_{\ell_2}, \quad Y = |\lambda|ADB < 1. \tag{7.2}$$

The operator $\overline{V}$ maps the space ℓ_2 onto itself in light of the inequality (7.2). □

Lemma 7.3. *Under the conditions* (1)-(4-b), $\overline{V}$ *defined by* (7.1) *is a contraction operator in the space* ℓ_2.

Proof. Considering formulas (7.1), we obtain the following if $\{\Theta_{nl,1}\}$ and $\{\Theta_{nl,2}\}$ are any functions in the space ℓ_2:

$$\|\overline{V}\Theta_{nl,1} - \overline{V}\Theta_{nl,2}\|_{\ell_2} \leqslant |\lambda| \sum_{i=0}^{l} |\omega_i F_{li}| \sum_{m=-M}^{M} |U_{mn}|\|\varpi_{im}(\Theta_{mi,1}) - \varpi_{im}(\Theta_{mi,2})\|_{\ell_2}.$$

Applying the conditions (1)-(4-a), the previous inequality has the following format:

$$\|\overline{V}\Theta_{nl,1} - \overline{V}\Theta_{nl,2}\|_{\ell_2} \leqslant Y\|\Theta_{nl,1} - \Theta_{nl,2}\|_{\ell_2}. \tag{7.3}$$

Under the condition $Y < 1$, inequality (7.3) displays the continuity of the operator $\overline{V}$ in the space ℓ_2, then $\overline{V}$ is a contraction operator. Therefore, by Banach fixed point theorem $\overline{V}$ has a unique fixed point which is the unique solution of the system of nonlinear algebraic equations (6.3). □

8. Examples

In this section, we study problems that are difficult to solve analytically and are important to researchers because they contain singular kernels of the logarithm type and Hilbert kernel. The numerical solution was obtained, and by getting the absolute error at different values of the time t, we proved the accuracy of the method used in the paper.

Example 8.1. Consider the following NMV-FIE:

$$\Theta(x,t) = f(x,t) + 0.5\int_0^t \int_{-1}^1 t^2\tau^2 \left(\ln|y-x|\right)^z \Theta^2(y,\tau)dyd\tau, \quad z = 1,2,\ldots, \tag{8.1}$$

where the function $f(x,t)$ is specified by laying $\Theta(x,t) = x^2t^2$ as an exact solution. With this formula, we get

$$X_m(x) = \frac{1}{\rho(z+1)}\sum_{k=0}^{z}(-1)^z(z+1)z(z-1)\cdots(z-k+1)\times\left[(m\rho+\rho-u)^2\left(\ln|m\rho+\rho-u|\right)^{z-k}\left\{1-\frac{1}{2^{k+1}}\right\}\right.$$
$$\left.-(m\rho-u)\left(\ln|m\rho-u|\right)^{z-k}\left\{(m\rho+\rho-u)-\frac{m\rho-u}{2^{k+1}}\right\}\right],$$

and

$$Y_m(x) = \frac{1}{\rho(z+1)}\sum_{k=0}^{z}(-1)^z(z+1)z(z-1)\cdots(z-k+1)\times\left[(m\rho+\rho-u)\left(\ln|m\rho+\rho-u|\right)^{z-k}\right.$$
$$\left.\times\left\{(u-\rho u)-\frac{m\rho+\rho-u}{2^{k+1}}\right\}+(m\rho-u)^2\left(\ln|m\rho-u|\right)^{z-k}\left\{1-\frac{1}{2^{k+1}}\right\}\right].$$

The Toeplitz matrix H_{mn} elements are provided by

$$H_{mn} = X_m(n\rho)+Y_{m-1}(n\rho) = \frac{\rho}{z+1}\sum_{k=0}^{z}(-1)^z(z+1)z(z-1)\cdots(z-k+1)\left\{1-\frac{1}{2^{k+1}}\right\}$$
$$\times\left[(m-n+1)^2\left(\ln|m-n+1|\rho\right)^{z-k}-2(m-n)^2\left(\ln|m-n|\rho\right)^{z-k}\right.$$
$$\left.+(m-n-1)^2\left(\ln|m-n-1|\rho\right)^{z-k}\right].$$

Given the matrix T_{mn}, the elements of its first column are

$$T_{n,-M} = Y_{-M-1}(n\rho) = \frac{\rho}{z+1}\sum_{k=0}^{z}(-1)^z(z+1)z(z-1)\cdots(z-k+1)\left[-(n+M)\left(\ln|n+M|\rho\right)^{z-k}\right.$$
$$\left.\times\left\{n+M+1-\frac{n+M}{2^{k+1}}\right\}+(n+M+1)^2\left(\ln|n+M+1|\rho\right)^{z-k}\left\{1-\frac{1}{2^{k+1}}\right\}\right],$$

while the elements of the last column of the matrix T_{mn} are provided by

$$T_{n,M} = X_M(n\rho) = \frac{\rho}{z+1}\sum_{k=0}^{z}(-1)^z(z+1)z(z-1)\cdots(z-k+1)\left[(M-n+1)^2\left(\ln|M-n+1|\rho\right)^{z-k}\right.$$
$$\left.\times\left\{1-\frac{1}{2^{k+1}}\right\}-(M-n)\left(\ln|M-n|\rho\right)^{z-k}\left\{M-n+1-\frac{M-n}{2^{k+1}}\right\}\right],$$

where, $-M \leqslant m,n \leqslant M$. By applying TMM with $M = 10,\ z = 5$ on the integral equation (8.1).

In Tables 1-4, for the position $x \in [-1, 1]$ and the time $t \in [0, 0.9]$, we have presented in the tables the exact solution of the equation (8.1) at different positions of the variable u and also the calculations were done at various times to know the behavior of the exact solution and through the presented method the approximate solution was obtained at the same positions and times and we obtained the amount of absolute error between the two solutions at the same studied points to know the efficiency of the presented technique for $M = 10$. In Figure 1, we computed exact solution, approximate solution, and errors of TMM with different values of x and $M = 10$ at $t = 0$.

Table 1: Exact solution, approximate solution, and errors for Example 8.1 at $M = 10$ and $t = 0$.

x	Exact solution	Approximate solution	Errors
-1.0	0	5.72476×10^{-14}	5.72476×10^{-14}
-0.8	0	4.17258×10^{-14}	4.17258×10^{-14}
-0.6	0	2.79024×10^{-14}	2.79024×10^{-14}
-0.4	0	7.48264×10^{-15}	7.48264×10^{-15}
-0.2	0	6.39214×10^{-15}	6.39214×10^{-15}
0.0	0	1.47298×10^{-15}	1.47298×10^{-15}
0.2	0	6.45827×10^{-15}	6.45827×10^{-15}
0.4	0	7.14025×10^{-15}	7.14025×10^{-15}
0.6	0	2.67359×10^{-14}	2.67359×10^{-14}
0.8	0	4.52098×10^{-14}	4.52098×10^{-14}
1.0	0	5.54109×10^{-14}	5.54109×10^{-14}

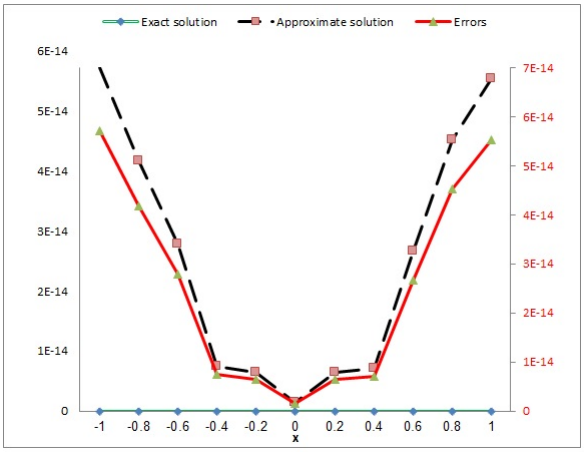

Figure 1: Exact solution, approximate solution, and errors of TMM at $t = 0$.

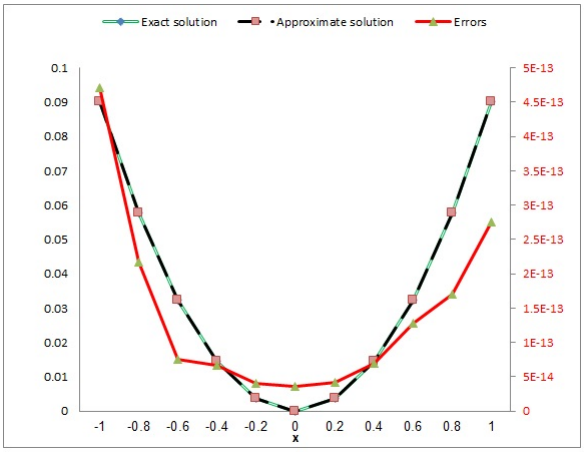

Figure 2: Exact solution, approximate solution, and errors of TMM at $t = 0.3$.

Table 2: Exact solution, approximate solution, and errors for Example 8.1 at $M = 10$ and $t = 0.3$.

x	Exact solution	Approximate solution	Errors
-1.0	0.09	0.09	4.71547×10^{-13}
-0.8	0.0576	0.0576	2.17206×10^{-13}
-0.6	0.0324	0.0324	7.49548×10^{-14}
-0.4	0.0144	0.0144	6.58412×10^{-14}
-0.2	0.0036	0.0036	4.08214×10^{-14}
0.0	0	3.52741×10^{-14}	3.52741×10^{-14}
0.2	0.0036	0.0036	4.21867×10^{-14}
0.4	0.0144	0.0144	6.97210×10^{-14}
0.6	0.0324	0.0324	1.20741×10^{-13}
0.8	0.0576	0.0576	1.69547×10^{-13}
1.0	0.09	0.09	2.00748×10^{-13}

In Figure 2, we computed exact solution, approximate solution, and errors of TMM with different values of x and $M = 10$ at $t = 0.3$.

Table 3: Exact solution, approximate solution, and errors for Example 8.1 at $M = 10$ and $t = 0.6$.

x	Exact solution	Approximate solution	Errors
-1.0	0.36	0.36	1.00758×10^{-11}
-0.8	0.2304	0.2304	4.17526×10^{-12}
-0.6	0.1296	0.1296	7.49823×10^{-13}
-0.4	0.0576	0.0576	5.71867×10^{-13}
-0.2	0.0144	0.0144	4.08467×10^{-13}
0.0	0	2.57129×10^{-13}	2.57129×10^{-13}
0.2	0.0144	0.0144	3.97287×10^{-13}
0.4	0.0576	0.0576	5.17592×10^{-13}
0.6	0.1296	0.1296	4.10564×10^{-12}
0.8	0.2304	0.2304	4.51725×10^{-12}
1.0	0.36	0.36	1.85424×10^{-11}

In Figure 3, we computed exact solution, approximate solution, and errors of TMM with different values of x and $M = 10$ at $t = 0.6$.

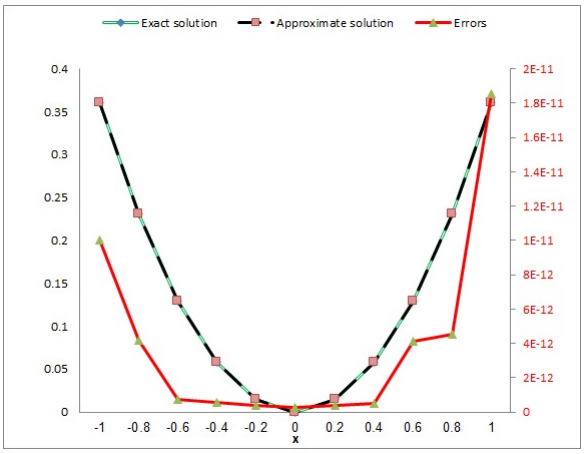

Figure 3: Exact solution, approximate solution, and errors of TMM at $t = 0.6$.

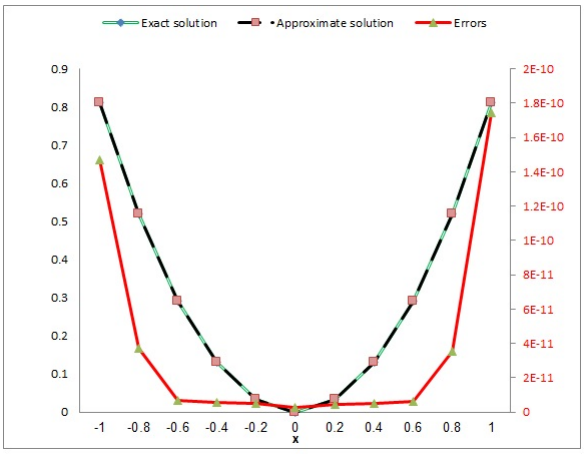

Figure 4: Exact solution, approximate solution, and errors of TMM at $t = 0.9$.

Table 4: Exact solution, approximate solution, and errors for Example 8.1 at $M = 10$ and $t = 0.9$.

x	Exact solution	Approximate solution	Errors
-1.0	0.81	0.81	1.47238×10^{-10}
-0.8	0.5184	0.5184	3.69524×10^{-11}
-0.6	0.2916	0.2916	6.58214×10^{-12}
-0.4	0.1296	0.1296	5.47238×10^{-12}
-0.2	0.0324	0.0324	4.71589×10^{-12}
0.0	0	2.47286×10^{-12}	2.47286×10^{-12}
0.2	0.0324	0.0324	4.58236×10^{-12}
0.4	0.1296	0.1296	5.14720×10^{-12}
0.6	0.2916	0.2916	6.21856×10^{-12}
0.8	0.5184	0.5184	3.54289×10^{-11}
1.0	0.81	0.81	1.75321×10^{-10}

In Figure 4, we computed exact solution, approximate solution, and errors of TMM with different

values of x and $M = 10$ at $t = 0.9$.

Example 8.2. Consider the following MV-FIE:

$$\Theta(x,t) = f(x,t) + \int_0^t \int_{-\pi}^{\pi} t\sin(\tau)\cot\left(\frac{|y-x|}{2}\right)\Theta(y,\tau)dyd\tau, \tag{8.2}$$

where the condition $\Theta(\pm\pi,0) = 0$ and the function $f(x,t)$ is specified by laying $\Theta(x,t) = (0.0.3+x)\sin(t)$ as an exact solution,

$$\int x^q \cot x dx = \sum_{k=0}^{\infty} \frac{(-1)^k 2^{2k} B_{2k}}{(q+2k)(2k)!} xq + 2k, \quad q \geqslant 1, |x| < \pi,$$

where the Bernoulli numbers are B_{2k}, one obtains

$$X_m(x) = \frac{1}{\rho}\left[2(m\rho+\rho-x)\ln\left|\sin\frac{m\rho+\rho-x}{2}\right| - 2(m\rho+\rho-x)\ln\left|\sin\frac{m\rho-x}{2}\right| - 4\sum_{k=0}^{\infty}\frac{(-1)^k B_{2k}}{2(1+2k)(2k)!}\left((m\rho+\rho-x)^{1+2k} - (m\rho-x)^{1+2k}\right)\right],$$

and

$$Y_m(x) = \frac{1}{\rho}\left[-2(m\rho-x)\ln\left|\sin\frac{m\rho+\rho-x}{2}\right| + 2(m\rho-x)\ln\left|\sin\frac{m\rho-x}{2}\right| + 4\sum_{k=0}^{\infty}\frac{(-1)^k B_{2k}}{2(1+2k)(2k)!}\left((m\rho+\rho-x)^{1+2k} - (m\rho-x)^{1+2k}\right)\right].$$

The Toeplitz matrix H_{mn} elements are provided by

$$H_{mn} = X_m(n\rho) + Y_{m-1}(n\rho) = 2(m-n+1)\ln\left|\sin\frac{\rho(m+n-1}{2}\right| - 4\sum_{k=0}^{\infty}\frac{(-1)^k\rho^{2k}B_{2k}}{2(1+2k)(2k)!}\left((m-n+1)^{1+2k} - 2(m-n)^{1+2k} + (m-n-1)^{1+2k}\right) - M + 1 \leqslant n, \quad m \leqslant M+1.$$

By applying the TMM with $M = 20$, $z = 5$ on the integral equation (8.2). In Tables 5-8, for $x \in [-\pi,\pi]$, $t = \{0.003, 0.05, 0.4, 0.8\}$, the exact solution, the approximate solution and the errors of TMM of (8.2) are calculated for $M = 20$.

Table 5: Exact solution, approximate solution, and errors for Example 8.2 at $M = 20$ and $t = 0.003$.

x	Exact solution	Approximate solution	Errors
$-\pi$	-0.008524765	-0.008524765	4.01427×10^{-19}
$-9\pi/10$	-0.007582289	-0.007582289	3.57217×10^{-19}
$-7\pi/10$	-0.005697336	-0.005697336	1.24038×10^{-19}
$-\pi/2$	-0.003812383	-0.003812383	3.94238×10^{-20}
$-3\pi/10$	-0.001927430	-0.001927430	3.75867×10^{-20}
$-\pi/10$	-4.24777×10^{-5}	-4.24777×10^{-5}	3.54864×10^{-20}
$\pi/10$	0.001842475	0.001842475	3.52741×10^{-20}
$3\pi/10$	0.003727428	0.003727428	3.72641×10^{-20}
$\pi/2$	0.005612381	0.005612381	3.94207×10^{-20}
$7\pi/10$	0.007497333	0.007497333	1.33547×10^{-19}
$9\pi/10$	0.009382286	0.009382286	3.74058×10^{-19}
π	0.010324762	0.010324762	1.23806×10^{-18}

In Figure 5, we computed exact solution, approximate solution, and errors of TMM with different values of x and M = 20 at t = 0.003.

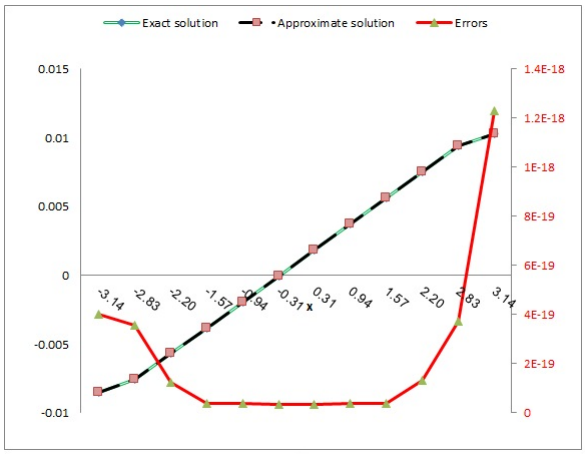

Figure 5: Exact solution, approximate solution, and errors of TMM at t = 0.003.

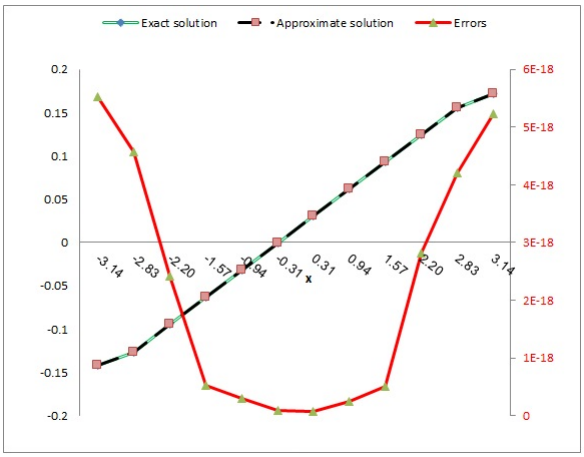

Figure 6: Exact solution, approximate solution, and errors of TMM at t = 0.05.

Table 6: Exact solution, approximate solution, and errors for Example 8.2 at M = 20 and t = 0.05.

x	Exact solution	Approximate solution	Errors
$-\pi$	-0.142020440	-0.142020440	5.53847×10^{-18}
$-9\pi/10$	-0.126319021	-0.126319021	4.58361×10^{-18}
$-7\pi/10$	-0.094916183	-0.094916183	2.41065×10^{-18}
$-\pi/2$	-0.063513345	-0.063513345	5.32864×10^{-19}
$-3\pi/10$	-0.032110507	-0.032110507	2.98613×10^{-19}
$-\pi/10$	-0.000707668	-0.000707668	8.34762×10^{-20}
$\pi/10$	0.030695170	0.030695170	8.11675×10^{-20}
$3\pi/10$	0.062098008	0.062098008	2.54762×10^{-19}
$\pi/2$	0.093500846	0.093500846	5.00741×10^{-19}
$7\pi/10$	0.124903684	0.124903684	2.81375×10^{-18}
$9\pi/10$	0.156306523	0.156306523	4.20964×10^{-18}
π	0.172007942	0.172007942	5.24768×10^{-18}

In Figure 6, we computed exact solution, approximate solution, and errors of TMM with different values of x and M = 20 at t = 0.05.

Table 7: Exact solution, approximate solution, and errors for Example 8.2 at M = 20 and t = 0.4.

x	Exact solution	Approximate solution	Errors
$-\pi$	-1.106568301	-1.106568301	4.72648×10^{-17}
$-9\pi/10$	-0.984228920	-0.984228920	2.75234×10^{-17}
$-7\pi/10$	-0.739550160	-0.739550160	5.24964×10^{-18}
$-\pi/2$	-0.494871399	-0.494871399	3.52764×10^{-18}
$-3\pi/10$	-0.250192638	-0.250192638	1.57342×10^{-18}
$-\pi/10$	-0.005513878	-0.005513878	3.85376×10^{-19}
$\pi/10$	0.239164883	0.239164883	3.47852×10^{-19}
$3\pi/10$	0.483843644	0.483843644	1.27649×10^{-18}
$\pi/2$	0.728522404	0.728522404	3.35967×10^{-18}
$7\pi/10$	0.973201165	0.973201165	1.44238×10^{-17}
$9\pi/10$	1.217879926	1.217879926	2.98346×10^{-17}
π	1.340219306	1.340219306	4.32879×10^{-17}

In Figure 7, we computed exact solution, approximate solution, and errors of TMM with different values of x and $M = 20$ at $t = 0.4$. In Figure 8, we computed exact solution, approximate solution, and errors of TMM with different values of x and $M = 20$ at $t = 0.8$.

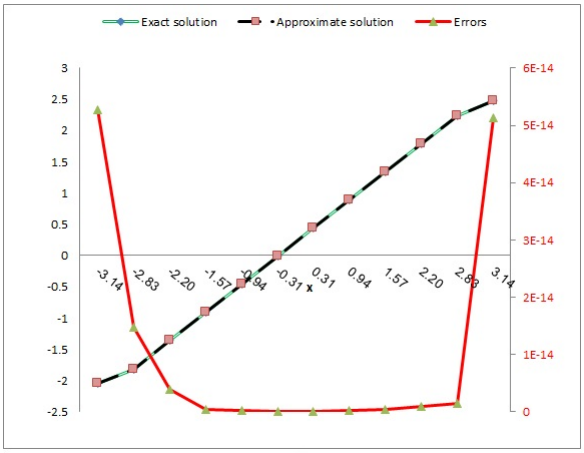

Figure 7: Exact solution, approximate solution, and errors of TMM at $t = 0.4$.

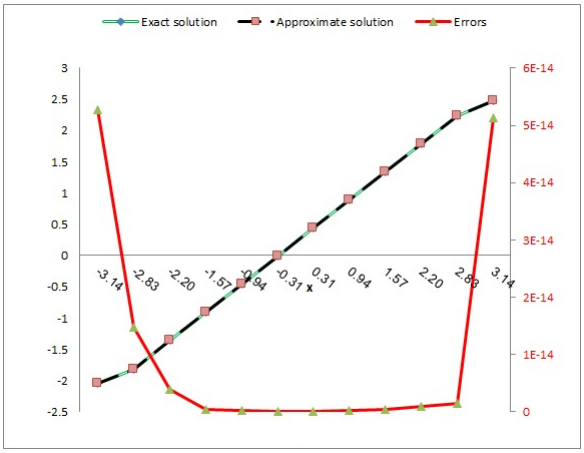

Figure 8: Exact solution, approximate solution, and errors of TMM at $t = 0.8$.

Table 8: Exact solution, approximate solution, and errors for Example 8.2 at $M = 20$ and $t = 0.8$.

x	Exact solution	Approximate solution	Errors
$-\pi$	-2.038433798	-2.038433798	5.27413×10^{-14}
$-9\pi/10$	-1.813069735	-1.813069735	1.47623×10^{-14}
$-7\pi/10$	-1.362341610	-1.362341610	3.87627×10^{-15}
$-\pi/2$	-0.911613485	-0.911613485	4.75632×10^{-16}
$-3\pi/10$	-0.460885360	-0.460885360	2.54368×10^{-16}
$-\pi/10$	-0.010157235	-0.010157235	4.52678×10^{-17}
$\pi/10$	0.440570890	0.440570890	4.27608×10^{-17}
$3\pi/10$	0.891299015	0.891299015	2.68537×10^{-16}
$\pi/2$	1.342027140	1.342027140	4.68204×10^{-16}
$7\pi/10$	1.792755265	1.792755265	1.01769×10^{-15}
$9\pi/10$	2.243483390	2.243483390	1.47398×10^{-15}
π	2.468847452	2.468847452	5.14938×10^{-14}

9. Remarks on numerical analysis and its application

From the above work, we can deduce the following.

1. NMV-FIE (1.1) has a unique solution $\Theta(x, t)$ in the Banach space $L_2(\Omega) \times C[0, T]$, under some conditions.
2. NMV-FIEs with different singular kernels are usually difficult to solve analytically, then it is required to obtain the approximate solutions.
3. The results in this paper show that these methods are effective and easy to implement.
4. For Example 8.1, it is observable that the error is 1.47298×10^{-15} at $M = 10$, the time $t = 0$, and $x = 0$ but at the same point, the error increases for the time $t = 0.9$ and becomes 2.47286×10^{-12}, also at the time $t = 0$ and point $x = -1$, the error is 5.72476×10^{-14} while for $t = 0.9$ at the same point, the error becomes 1.75321×10^{-10}, this means that if the time is increased, then the error is also increasing. This has also been noted in the rest of the tables. As the value of x increases the error increases.

5. From Example 8.2, the minimum value of the error in the linear case is 3.52741×10^{-20} at $x = \pi/10$ for $M = 20$ and $t = 0.003$, while the maximum value of the error in the linear case is 5.27413×10^{-14} at $x = -\pi$ for $M = 20$ and $t = 0.8$, this means that the maximum error is at $x = \pm\pi$, and when the values of T are increasing, the error values increase slowly.

10. General conclusion

From the above work, we can deduce the following.

1. Many natural phenomena can be represented in the form of a non-linear integral equation in position and time.
2. These equations have been assumed to have a general singular kernel, from which many special cases can be derived, fully explained in Section 2.
3. The kernel in the science of integral equations refers to the properties of the materials used, whether they are elastic or liquid.
4. Continuous integral equations, whether linear or nonlinear, can be solved in many ways. These methods may be semi-analytical methods or explicit numerical methods.
5. In the case of singular integral equations, there are two methods for solving them: Nystrom multiplication method, which is a very long method in its analysis to convert the integral system into a linear system. The other method used is the Toeplitz matrix method.
6. The Toeplitz matrix method is characterized by the ease of converting singular integrals into non-singular integrals that can be easily calculated. It is also characterized by the speed of converting the integral system into an algebraic system that can be studied.
7. It is also characterized by the fact that all singular cases that were previously studied in various papers can be studied here as applications of the method (see Section 2).

Acknowledgments

The authors would like to thank the Editorial Board and the reviewers for their constructive suggestions and comments that greatly improved the final version of the paper.

Funding

This research is funded by the Deanship of Graduate Studies and Scientific Research at Jouf University through the Fast-Track Research Funding Program.

Future work

The authors will interest in solving the same formula of equation (1.1) with Phase-lag constant q in time:

$$\Theta(u, t+q) = f(u, t+q) + \lambda \int_0^{t+q} \int_\Omega F(t+q, \tau) k(|x-y|) \varpi(\tau, y, \Theta(y, \tau)) dy d\tau, \quad 0 < q << 1.$$

References

[1] M. A. Abdel-Aty, M. E. Nasr, *Application of Adomian polynomials for solving nonlinear integro-differential equations*, J. Math. Comput. Sci., **32** (2024), 188–200. 1
[2] W. Abdul-Majid, *Linear and Nonlinear integral equations: Methods and Applications*, Springer, New York, (2011). 1
[3] S. A. Abusalim, M. A. Abdou, M. A. Abdel-Aty, M. E. Nasr, *Hybrid functions approach via nonlinear integral equations with symmetric and nonsymmetrical kernel in two dimensions*, Symmetry, **15** (2023), 19 pages. 1
[4] J. Alahmadi, M. A. Abdou, M. A. Abdel-Aty, *Analytical and Numerical Approaches via Quadratic Integral Equations*, Axioms, **13** (2024), 20 pages. 1, 6

[5] J. Alahmadi, M. A. Abdou, M. A. Abdel-Aty, *Analytical and numerical treatment of a nonlinear Fredholm integral equation in two dimensions*, J. Appl. Math. Comput., **71** (2025), 1693–1719. 1

[6] A. M. Al-Bugami, *Numerical treating of mixed integral equation two-dimensional in surface cracks in finite layers of materials*, Adv. Math. Phys., **2022** (2022), 12 pages. 1

[7] A. Al-Bugami, J. Al-Juaid, *Runge-Kutta method and Bolck by Block method to solve nonlinear Fredholm-Volterra integral equation with continuous kernel*, J. Appl. Math. Phys., **82** (2020), 2043–2054. 1

[8] V. M. Aleksandov, E. V. Kovalenko, *Problems in Mechanics Media with Mixed Boundary Conditions*, Nauka, Moscow, (1986). 1

[9] S. E. Alhazmi, *New model for solving mixed integral equation of the first kind with generalized potential kernel*, J. Math. Res., **9** (2017), 18–29. 1

[10] M. Basseem, *Degenerate method in mixed nonlinear three dimensions integral equation*, Alex. Eng. J., **58** (2019), 387–392. 1

[11] H. Brunner, *Collocation methods for Volterra integral and related functional differential equations*, Cambridge University Press, Cambridge, (2004). 1

[12] M. V. K. Chari, S. Salon, *Numerical Methods in Electromagnetism*, Academic Press, (1999). 1

[13] Z. Chen, W. Jiang, *An approximate solution for a mixed linear Volterra-Fredholm integral equation*, Appl. Math. Lett., **25** (2012), 1131–1134. 1

[14] P. Das, G. Nelakanti, *Convergence analysis of Legendre spectral Galerkin method for Volterra-Fredholm-Hammerstein integral equations*, Springer, New Delhi, **143** (2015), 3–15. 1

[15] L. M. Delves, J. L. Mohamed, *Computational methods for integral equations*, Cambridge University Press, Cambridge, (1985). 1

[16] S. Deniz, *Optimal perturbation iteration technique for solving nonlinear Volterra-Fredholm integral equations*, Math. Methods Appl. Sci., **47** (2024), 10595–10601. 1

[17] C. Dong, Z. Chen, W. Jiang, *A modified homotopy perturbation method for solving the nonlinear mixed Volterra-Fredholm integral equation*, J. Comput. Appl. Math., **239** (2013), 359–366. 1

[18] Z. El Majouti, R. El Jid, A. Hajjaj, *Numerical solution for three-dimensional nonlinear mixed Volterra-Fredholm integral equations via modified moving least-square method*, Int. J. Comput. Math., **99** (2022), 1849–1867. 1

[19] M. Erfanian, H. Zeidabadi, *Using of Bernstein spectral Galerkin method for solving of weakly singular Volterra-Fredholm integral equations*, Math. Sci. (Springer), **12** (2018), 103–109. 1

[20] J. Gao, M. Condon, A. Iserles, *Spectral computation of highly oscillatory integral equations in laser theory*, J. Comput. Phys., **395** (2019), 351–381. 1

[21] A. Georgieva, S. Hristova, *Homotopy analysis method to solve two-dimensional nonlinear Volterra-Fredholm fuzzy integral equations*, Fractal Fract., **4** (2020), 14 pages. 1

[22] Z. Gouyandeh, T. Allahviranloo, A. Armand, *Numerical solution of nonlinear Volterra-Fredholm-Hammerstein integral equations via tau-collocation method with convergence analysis*, J. Comput. Appl. Math., **308** (2016), 435–446. 1

[23] B. H. Hashemi, M. Khodabin, K. Maleknejad, *Numerical method for solving linear stochastic Itô-Volterra integral equations driven by fractional Brownian motion using hat functions*, Turkish J. Math., **41** (2017), 611–624. 1

[24] H. B. Jebreen, *On the multiwavelets Galerkin solution of the Volterra-Fredholm integral equations by an efficient algorithm*, J. Math., **2020** (2020), 10 pages. 1

[25] M. Lienert, R. Tumulka, *A new class of Volterra-type integral equations from relativistic quantum physics*, J. Integral Equations Appl., **31** (2019), 535–569. 1

[26] N. Madbouly, *Solutions of Hammerstein integral equations arising from chemical reactor theory*, University of Strathclyde, PhD. thesis, (1996). 1

[27] R. T. Matoog, M. A. Abdou, M. A. Abdel-Aty, *New algorithms for solving nonlinear mixed integral equations*, AIMS Math., **8** (2023), 27488–27512. 1

[28] S. Micula, *An iterative numerical method for Fredholm-Volterra integral equations of the second kind*, Appl. Math. Comput., **270** (2015), 935–942. 1

[29] S. Micula, *On Some Iterative Numerical Methods for Mixed Volterra-Fredholm Integral Equations*, Symmetry, **11** (2019), 10 pages. 1

[30] F. Mirzaee, E. Hadadiyan, *Applying the modified block-pulse functions to solve the three-dimensional Volterra-Fredholm integral equations*, Appl. Math. Comput., **265** (2015), 759–767. 1

[31] F. Mirzaee, N. Samadyar, *Convergence of 2D-orthonormal Bernstein collocation method for solving 2D-mixed Volterra-Fredholm integral equations*, Trans. A. Razmadze Math. Inst., **172** (2018), 631–641. 1

[32] F. Mirzaee, E. Hadadiyan, *Using operational matrix for solving nonlinear class of mixed Volterra-Fredholm integral equations*, Math. Methods Appl. Sci., **40** (2017), 3433–3444. 1

[33] M. E. Nasr, M. A. Abdel-Aty, *A new techniques applied to Volterra-Fredholm integral equations with discontinuous kernel*, J. Comput. Anal. Appl., **29** (2021), 11–24. 1

[34] S. Noeiaghdam, S. Micula, *A novel method for solving second kind Volterra integral equations with discontinuous kernel*, Mathematics, **9** (2021), 12 pages. 1

[35] C. Nwaigwe, S. Micula, *Fast and Accurate Numerical Algorithm with Performance Assessment for Nonlinear Functional Volterra Equations*, Fractal Fract., **7** (2023), 15 pages. 1

[36] S. Paul, M. M. Panja, B. N. Mandal, *Use of Legendre multiwavelets to solve Carleman type singular integral equations*,

Appl. Math. Model., **55** (2018), 522–535. 1
[37] G. Y. Popov, *Contact problems for a linearly deformable foundation*, Vishcha Schola, Kiev-Odessa, (1982). 1
[38] M. A. Ramadan, H. S. Osheba, A. R. Hadhoud, *A numerical method based on hybrid orthonormal Bernstein and improved block-pulse functions for solving Volterra-Fredholm integral equations*, Numer. Methods Partial Differ. Equ., **39** (2023), 268–280. 1
[39] A. M. Rocha, J. S. Azevedo, S. P. Oliveira, M. R. Correa, *Numerical analysis of a collocation method for functional integral equations*, Appl. Numer. Math., **134** (2018), 31–45. 1
[40] N. H. Sweilam, A. M. Nagy, I. K. Youssef, M. M. Mokhtar, *New spectral second kind Chebyshev wavelets scheme for solving systems of integro-differential equations*, Int. J. Appl. Computat. Math., **3** (2017), 333–345. 1
[41] A. N. Tikhonov, V. Y. Arsenin, *Solutions of ill-posed problems*, V. H. Winston & Sons, Washington, DC; John Wiley & Sons, New York-Toronto-London, (1977). 1
[42] X. Wang, *A new wavelet method for solving a class of nonlinear Volterra-Fredholm integral equations*, Abstr. Appl. Anal., **2014** (2014), 6 pages. 1
[43] Q. Wang, K. Wang, S. Chen, *Least squares approximation method for the solution of Volterra-Fredholm integral equations*, J. Comput. Appl. Math., **272** (2014), 141–147. 1
[44] K. F. Warnick, *Numerical analysis for electromagnetic integral equations*, Artech House, (2008). 1